

The zinc-finger protein CNBP is required for forebrain formation in the mouse

Wei Chen^{1,2}, Yuqiong Liang¹, Wenjie Deng¹, Ken Shimizu¹, Amir M. Ashique^{1,2}, En Li³ and Yi-Ping Li^{1,2,*}

¹Department of Cytokine Biology, The Forsyth Institute, Boston, MA 02115, USA

²Harvard-Forsyth Department of Oral Biology, Harvard School of Dental Medicine, Boston, MA 02115, USA

³Cardiovascular Research Center, Massachusetts General Hospital, Department of Medicine, Harvard Medical School, Charlestown, MA 02129, USA

*Author for correspondence (e-mail: ypli@forsyth.org)

Accepted 19 December 2002

SUMMARY

Mouse mutants have allowed us to gain significant insight into axis development. However, much remains to be learned about the cellular and molecular basis of early forebrain patterning. We describe a lethal mutation mouse strain generated using promoter-trap mutagenesis. The mutants exhibit severe forebrain truncation in homozygous mouse embryos and various craniofacial defects in heterozygotes. We show that the defects are caused by disruption of the gene encoding cellular nucleic acid binding protein (CNBP); *Cnbp* transgenic mice were able to rescue fully the mutant phenotype. *Cnbp* is first expressed in the anterior visceral endoderm (AVE) and, subsequently, in the anterior definitive endoderm (ADE), anterior neuroectoderm (ANE), anterior mesendoderm

(AME), headfolds and forebrain. In *Cnbp*^{-/-} embryos, the visceral endoderm remains in the distal tip of the conceptus and the ADE fails to form, whereas the node and notochord form normally. A substantial reduction in cell proliferation was observed in the anterior regions of *Cnbp*^{-/-} embryos at gastrulation and neural-fold stages. In these regions, *Myc* expression was absent, indicating CNBP targets *Myc* in rostral head formation. Our findings demonstrate that *Cnbp* is essential for the forebrain induction and specification.

Key words: CNBP, Retroviral insertional mutagenesis, Forebrain patterning, AVE, ADE, ANE, Cell proliferation defects, *Myc* expression

INTRODUCTION

Craniofacial abnormalities affect hundreds of thousands of children each year and result in physical, emotional and economic hardships for affected individuals and their families (Cohen, 1993). The isolation of genes underlying mouse mutants that resemble the human syndromes promises to identify many important players in normal and abnormal craniofacial development (Jabs et al., 1993; Dattani et al., 1998). Similarly, gene knockout techniques have proved to be powerful tools for identifying the molecular regulation of many developmental processes. For example, genes such as *Lim1* (*Lhx1* – Mouse Genome Informatics) (Shawlot and Behringer, 1995), *Otx2* (Matsuo et al., 1995; Acampora et al., 1995), *Smad2* (Waldrup et al., 1998; Nomura and Li, 1998), *Nodal* (Brennan et al., 2001), *Foxh1* (Hoodless et al., 2001; Yamamoto et al., 2001), *Arkadia* (Episkopou et al., 2001), *Hex* (Martinez Barbera et al., 2000), *Oto* (Zoltewicz et al., 1999), *Hesx1* (Dattani et al., 1998) and *Dkk1* (Mukhopadhyay et al., 2001; Shawlot et al., 1999; Yamamoto et al., 2001) have been demonstrated to be essential for normal head development by targeted gene disruption in mice. However, studies using such knockout techniques are limited to known genes. Through retroviral insertional mutagenesis and genetic screening approaches, we have identified a null-mutant mouse strain with complete forebrain truncation. Heterozygous mutants survive

to birth with various craniofacial abnormalities, including the absence of the lower jaw and eyes. The mutated gene has been determined to be that encoding the cellular nucleic acid binding protein (CNBP); this was confirmed by transgenic rescue.

The *Cnbp* gene encodes a 19 kDa protein containing seven tandem zinc-finger repeats of 14 amino acids (Covey, 1986). The amino acid sequence of CNBP is highly conserved; the sequence of human CNBP is 94.1% identical to that of *Xenopus laevis* (Flink et al., 1998), 99% identical to that of the chick (van Heumen et al., 1997) and 100% identical to the mouse protein. Despite its discovery over a decade ago, little is known about CNBP function. CNBP was initially postulated to function as a negative-transcription regulator in the coordinate control of cholesterol metabolism (Rajavashisth et al., 1989) but this has not been confirmed (Ayala-Torres et al., 1994; Warden et al., 1994). CNBP was subsequently shown to be a single strand-specific DNA-binding protein that interacts with the sequence CCCTCCCCA (termed the CT element), a segment of DNA that enhances *Myc* promoter activity (Michelotti et al., 1995). Recently, Konicek et al. reported that CNBP upregulates CSF1 promoter activity in a tissue-specific manner through specific DNA-binding protein interactions (Konicek et al., 1998). Expression studies during embryogenesis, determined that *Xenopus* CNBP (*XCNBP*) was located in the ectoderm, endoderm and mesoderm during early development, and in a wide variety of cell types during late *Xenopus* embryogenesis

(Flink et al., 1998). De Dominicis et al. further reported that, in *Xenopus* embryos, *CNBP* mRNA accumulation during development decreases before the mid-blastula stage and increases again thereafter (De Dominicis et al., 2000). Although the *in vivo* role and expression pattern of CNBP in mammalian development remains unclear, the extraordinary level of conservation and the expression pattern in *Xenopus* embryos suggest a potentially important role for CNBP during early embryonic development across different species.

The biological events that control anterior and posterior patterning in vertebrate embryos is one of the most intriguing questions to challenge biologists. Recent evidence from studies in the mouse suggests that anterior patterning precedes gastrulation (Beddington and Robertson, 1999). In mouse embryos, an increasing number of genes have been identified that are expressed in the anterior visceral endoderm (AVE) before, or coincident with, the start of gastrulation (Lu et al., 2001). Mutations in a number of transcription factor genes, such as *Otx2*, *Lim1*, *Hex* and *Hesx1*, that are first expressed in the AVE and, subsequently, in the node and node derivatives, affect anterior development and exhibit anterior truncation. The AVE region is located at the distal tip of the conceptus prior to primitive streak formation, and, subsequently, undergoes a morphogenetic movement toward the proximal/anterior region. These movements have been proposed to be extremely important for the anteroposterior patterning of the embryo (Beddington and Robertson, 1999). For example, in *Otx2*^{-/-} embryos at egg cylinder stages, the posterior rotation of epiblast seems to occur normally but the AVE remains distal (Acampora et al., 1998), and the resulting embryos lack midbrain and forebrain. The AVE cells have been suggested to detach from the epithelial sheet and move toward the anterior region (Kimura et al., 2000). It is currently not understood what mechanisms drive either of these processes.

The mouse node structure is homologous to the Spemann's organizer in *Xenopus*. It gives rise to a similar repertoire of embryonic tissues: prechordal mesoderm, notochord and gut endoderm (Beddington, 1981; Beddington, 1994; Lawson et al., 1991). However, it is unable to induce secondary anterior structures even when node precursor cells are transplanted from an early gastrula stage (Tam and Steiner, 1999). AVE appears to repress posterior signals in the epiblast. However, it is unable to pattern the neuroectoderm or cause formation of anterior embryonic structures (Lu et al., 2001; Moon and Kimelman, 1998; Piotrowska and Zernicka-Goetz, 2001). The anterior definitive endoderm (ADE) arises from the anterior streak region before node formation and notochord extension, and moves anteriorly to displace the AVE and underlie the prospective neuroectoderm during gastrulation (Lawson and Pedersen, 1987; Tam and Beddington, 1992; Lu et al., 2001). The ADE expresses many of the same genes as the AVE, such as *Hex* and *Cer1*, making it an attractive candidate tissue from the anterior streak for patterning the anterior epiblast (Martinez Barbera et al., 2000; Lu et al., 2001). Although, the AVE, ADE and node tissues are essential for head development, the precise function and interaction of these three tissues remain unresolved. We report a new mouse mutant, generated by retroviral insertion into the locus of the *Cnbp* gene, that displays impaired anterior movement of AVE, lack of both ADE and anterior neuroectoderm (ANE) tissues, and forebrain truncation.

MATERIALS AND METHODS

Generation of the *Cnbp* mutant mouse strain

The *Cnbp* mutant mouse strain, also termed A8, was generated as described (Harbers et al., 1996). Briefly, J1 embryonic stem (ES) cells (Li et al., 1992) were grown on a monolayer of mytomycin C-treated Psi-2 cells producing mp 10 virus (Barklis et al., 1986) in ES cell culture medium containing 8 µg/ml polybrene. ES cell lines with a single-copy proviral genome were injected into BALB/c or C57BL/6J blastocysts, and injected embryos were then transferred into the uteri of pseudopregnant F1 (C57BL/6J×CBA) foster mothers as described (Li et al., 1992) to obtain transgenic lines. The *Cnbp* transgenic line was obtained by breeding a male chimera with a female C57BL/6J mouse. The *Cnbp* mutation was repeatedly backcrossed (>12 generations) onto the C57BL/6J inbred genetic background to improve phenotypic consistency. *Cnbp*^{+/-} inbred mice were intercrossed to produce *Cnbp*^{-/-} mice.

Molecular cloning

Initially, a genomic DNA fragment flanking the 5' end of the mp 10 provirus was cloned by inverse PCR. This fragment, designated 5' fA8 (see Fig. 1), was subcloned into the Bluescript vector (Stratagene). To obtain λ-phage clones representing the A8 locus from wild-type mice, a 129/Sv mouse genomic library in lambda FIXII (Stratagene) was screened with a radiolabeled probe derived from 5' fA8. Positive plaques were purified by three rounds of screening and sub-fragments from the λ clones were subcloned according to standard procedures. The physical map of the A8 locus shown in Fig. 1 was obtained by both sequence analyses of the plasmid clones and Southern blot analyses of restriction enzyme digested wild-type and mutant genomic DNA.

Genotype analysis

For genotyping, DNA was isolated from the yolk sac of dissected embryos or from the terminal tail region of adult animals and analyzed by PCR or by Southern blot using 5' fA8 as a probe (Fig. 1). Embryos were obtained from timed matings; the day of plug detection was counted as day 0.5 of gestation. The presence of a single 8 kb fragment indicates a homozygote genotype (Fig. 1). Oligonucleotide primers P1 (ATAGGACCCGTAGGTGTGCA), P2 (CTCTGAGTGATTGACTACCC) and P3 (AGTCTCTCCAGAATTGGGTC) were used to give diagnostic amplification products of 500 bp for the wild-type *Cnbp* allele and 300 bp for the disrupted *Cnbp* allele (Fig. 1). Data from this study were from C57/B6J inbred mice.

RNA preparation and analysis

Total cellular RNA was isolated from adult tissues and mouse embryos by the guanidinium isothiocyanate procedure. Extracted RNA was fractionated (15 µg per lane) by electrophoresis in 1% agarose gels containing formaldehyde and then transferred onto nylon membranes (Li et al., 1999). Blots were hybridized for 18–20 hours at 65°C in a standard hybridization solution without formamide (Li et al., 1999).

Histology

Embryos and tissues were fixed in 4% paraformaldehyde. Tissues were embedded in paraffin wax and sectioned at 7 µm. Sections were stained with Hematoxylin and Eosin according to standard procedures.

Immunostaining

Tissue section immunostaining was performed as described (Li et al., 1999) using anti-CNBP polyclonal anti-peptide antibodies raised against a 20 amino acid peptide from the C terminus of mouse CNBP (CYRCGESGHLARECTIEATA).

In situ hybridization

Whole-mount in situ hybridization was performed as described (Deng et al., 2001). The full-length mouse *Cnbp* cDNA was subcloned and

linearized with *NotI* and transcribed with T3-RNA polymerase. The Krox20 cDNA was linearized with *BamHI* and transcribed with T3-RNA polymerase. *En1* and *Hnf3b* cDNA were linearized and transcribed with T7-RNA polymerase. Other antisense probes used were for: *Myc*, *Mox1* (*Meox1* – Mouse Genome Informatics), *Otx2*, *Brachyury (T)*, *Hex*, *Lim1*, *Six3*, *Dkk1*, *Gsc*, *Hexx1* and *Cer1*. At least five embryos with the same genetic background were analyzed for each probe.

Transgenic rescue of forebrain defect in *Cnbp* mutants

Cnbp transgenic mice were used to rescue the forebrain truncation in *Cnbp* mutants. The transgenic vector construct that was used contained 10 kb of the CNBP promoter and 11 kb of the entire *Cnbp* gene. The vector DNA was linearized and used for pronuclear microinjection to obtain *Cnbp* transgenic mice. Transgenic (TG) mice were crossed to *Cnbp*^{+/-} mutants and the resultant progeny (TG/*Cnbp*^{+/-}) were backcrossed to *Cnbp*^{+/-} mice. Litters were examined at E9.5.

BrdU and TUNEL assays

BrdU incorporation and TUNEL assays were performed as described (Shen-Li et al., 2000). At least five embryos with the same genetic background were analyzed for each stage.

Transfection study

Transfection study was performed as described previously (He et al., 1998). Wild-type and *Cnbp*^{+/-} mutant embryonic fibroblasts (MEF) were isolated from E13.5 embryos in C57B1/6J and 129Sv hybrid background using 0.05% trypsin/EDTA digestion and then maintained in MEM/10% FBS. Wild-type and *Cnbp*^{+/-} mutant embryonic fibroblasts (MEF) were transfected with a *Myc* promoter-luciferase reporter plasmid or co-transfected with the luciferase reporter DNA and a mouse *Cnbp* expression plasmid (pCMV-CNBP) as described (He et al., 1998). The pCMV-CNBP was constructed by inserting the *Cnbp* cDNA under the transcriptional control of a CMV promoter in the pCDNA3.1 vector (Invitrogen). *Cnbp* cDNA was obtained by screening a day 17.5 mouse embryo cDNA library (Clontech). DNA co-transfections were performed in duplicate and repeated at least four times.

RESULTS

Retroviral insertional mutation of *Cnbp* is embryonically lethal and results in defects in anterior patterning

We have generated a mutant mouse strain (A8) that exhibits severe forebrain truncation and facial anomalies (Fig. 1A-E). The external morphological deficiencies were variable but limited to the forebrain, eyes and lower jaw. The A8 mutant mice were generated using retroviral insertional mutagenesis (Harbers et al., 1996). The 500 bp DNA fragment flanking the 5' LTR of the provirus was cloned by inverse PCR and designated 5' fA8 (Fig. 1L). When used as a probe on Southern blots, 5' fA8 hybridizes to a single 4 kb band in genomic DNA from wild-type mice (Fig. 1M), and an additional 8 kb band, resulting from the insertion of the provirus, in DNA from heterozygous animals, which was used for genotyping mice and embryos (Fig. 1M). Mutant embryos were also genotyped by PCR analysis (Fig. 1N). To ensure genetic uniformity for closely linked loci, heterozygous mice were backcrossed to C57BL/6J inbred strain 12 times. To define the role of *Cnbp* in mouse development, the offspring from intercrossed heterozygous (*Cnbp*^{+/-}) C57BL/6J inbred mice (*n*=12) were

Table 1. Genotype of mice resulting from *Cnbp* heterozygous intercrosses in C57BL/6J inbred mice

Stage	+/+	-/+	-/- (%)
E7.5	22	49	21 (23)
E8.5	43	77	38 (24)
E9.5	29	58	24 (22)
E10.5	27	40	14* (17)
Postpartum	32	51	0

*Embryos were either severely growth retarded or being resorbed.

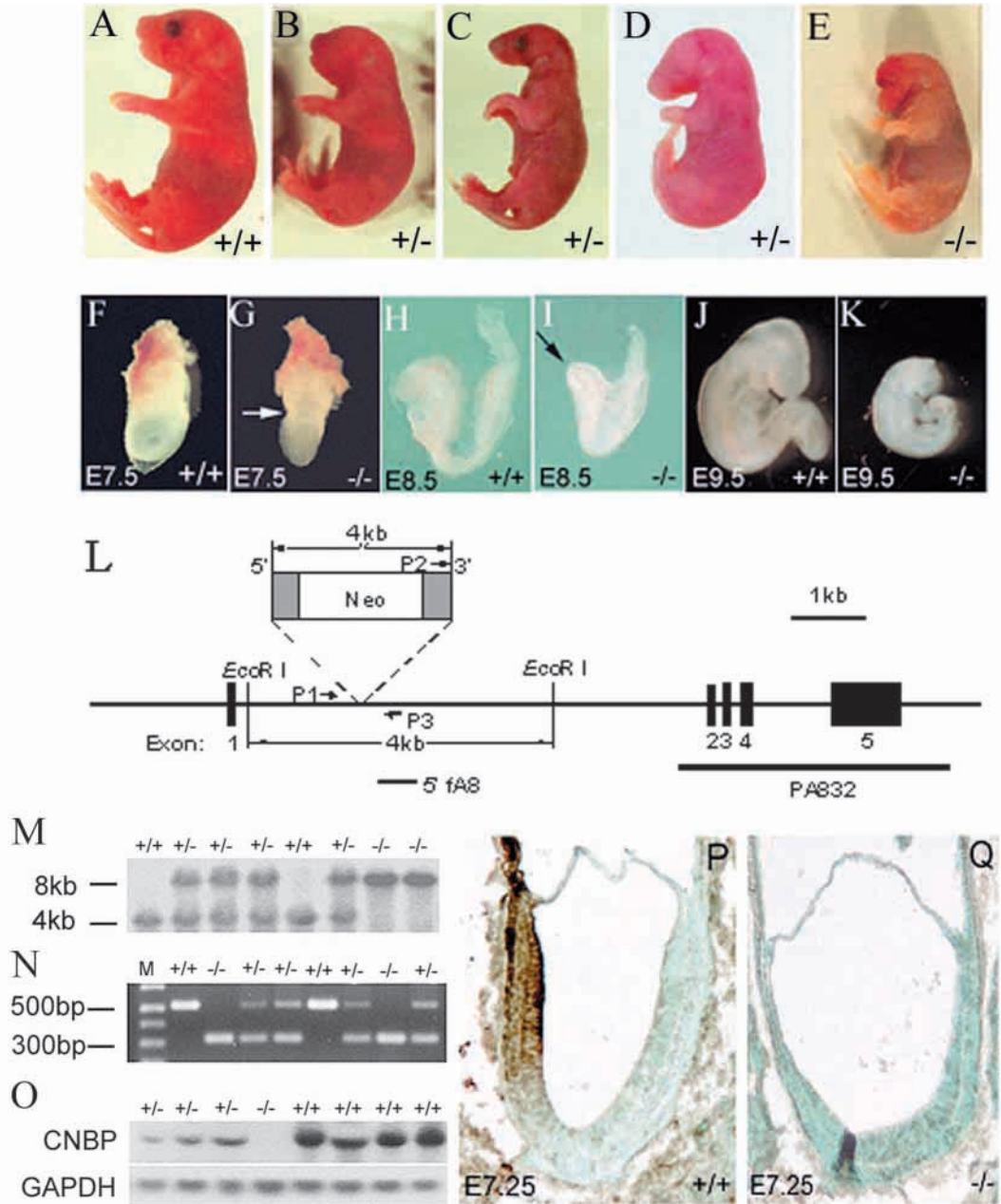
examined at various developmental stages. We found that A8 homozygous embryos had a severe forebrain truncation and died around E10.5 (Table 1). No A8 homozygous newborns were ever found. About 40% of heterozygous newborn mutants exhibited multiple defects, including growth retardation and craniofacial defects (e.g. a smaller mandible and complete lack of eyes), and died shortly after birth. The haploinsufficiency suggests that the *Cnbp* gene must be expressed above a threshold level to ensure normal development. The remaining heterozygous mice either grew normally to adulthood or had mild eye and skeleton defects (data not shown).

In order to identify the gene that is responsible for the mutation, additional genomic sequences flanking 5' fA8 were isolated by screening a λ -phage library of mouse genomic DNA with the 5' fA8 probe. The λ clones were dissected into subfragments and used as probes to hybridize to northern blots containing poly(A)⁺ RNA that was extracted from newborn mice. A 3.0 kb subfragment, designated PA832 (as shown in Fig. 1), hybridized to a 1.65 kb RNA transcript. Sequencing the PA832 fragment indicated that the proviral insertion created a mutation in the previously described *Cnbp* gene (Rajavashisth et al., 1989). In order to map the proviral integration site relative to the transcriptional unit of the *Cnbp* gene, the exon-intron junctions of the gene were identified by comparing *Cnbp* gene sequences with *Cnbp* cDNA sequences. The results summarized schematically in Fig. 1 indicate that the provirus was inserted into the first intron. To test whether the proviral insertion affected levels of *Cnbp* transcription, total RNA was isolated from E9.5 embryos (derived from *Cnbp* heterozygous mutant parents) and analyzed on northern blots. Compared with their wild-type littermates, the 1.65 kb *Cnbp* transcripts were significantly reduced in heterozygous embryos and could not be detected in homozygous embryos (Fig. 1O). In order to examine CNBP protein levels, immunostaining of tissue sections was performed using an anti-CNBP polyclonal anti-peptide. We found that, *Cnbp* was normally expressed in the ANE and ADE of E7.25 embryos (Fig. 1P) but was absent in E7.25 *Cnbp*^{+/-} mutant embryos (Fig. 1Q). These results indicate that the *Cnbp* mutation was a null mutation.

Morphological analysis showed that *Cnbp*^{+/-} mutant embryos were distinguishable from normal embryos. At E7.5, the abnormal-looking embryos were smaller than their normal littermates (Fig. 1F,G). A constriction was seen between the embryonic and extra-embryonic regions (Fig. 1G). A similar extra-embryonic/embryonic constriction was also observed in *Hnf3b* mutants (Ang and Rossant, 1994) and *Otx2* mutants (Ang et al., 1996) and to a lesser extent in *Lim1* mutants (Shawlot and Behringer, 1995). Truncations were also seen in the anterior neural folds at early somite stages (Fig. 1H,I) and in the anterior

Fig. 1. Retroviral insertional mutation of CNBP resulted in anterior patterning and craniofacial defects.

(A) Morphology of newborn wild-type mouse. (B) A heterozygote newborn mouse with a short snout and lacking eyes. (C,D) Heterozygotes with a smaller lower jaw (C) and missing eyes (D). (E) A homozygote lacking rostral head structures, including the entire forebrain. (F,G) As early as E7.5, a homozygous mutant embryo is smaller than its wild-type littermate. A constriction is observed between embryonic and extra-embryonic regions in *Cnbp*^{-/-} mutants (arrow in G). (H,I) By E8.5, forebrain truncation is evident in mutant embryo (arrow in I). (J,K) At E9.5, *Cnbp*^{-/-} embryos were smaller with forebrain truncations. (L) The integration site of the provirus in the *Cnbp* gene locus. The flanking sequence, 5' fA8, was cloned by inverse PCR. The *Cnbp* gene was cloned and characterized by using 5' fA8 as probe. The positions of the 5' fA8 probe and primers 1, 2 and 3 (P1, P2, and P3) for genotyping are shown. (M) Genotype analysis of *Cnbp* mutant mice by Southern blot. The presence of a single 4 kb fragment represents wild-type allele, while a larger 8 kb fragment, a result of the proviral insertion, represents a mutant allele. (N) Genotype analysis of E6.5 embryos by PCR demonstrates the recovery of wild-type (lanes 1, 5), heterozygous (lanes 3, 4, 6, 8) and homozygous embryos (lanes 2, 7). Primers P1 and P3 amplify a 500 bp wild-type fragment, whereas primers P2 (a Neo insertion-specific primer) and P3 together amplify a 300 bp mutant fragment. (O) Northern blot analysis of total RNA isolated from E9.5 whole embryos derived from *Cnbp*-heterozygous mutant parents. A 1.65 kb mRNA was detected in the wild-type and heterozygous embryos but was undetectable in the homozygous embryos using *Cnbp* cDNA as a probe. (P,Q) Immunostaining in tissue sections was performed, using an anti-CNBP polyclonal antibody, to examine CNBP protein levels in E7.25 wild-type and mutant embryos. CNBP protein was localized to the ANE and ADE of a wild-type embryo (brown staining in P) but was absent in the *Cnbp*^{-/-}-mutant embryo (Q).



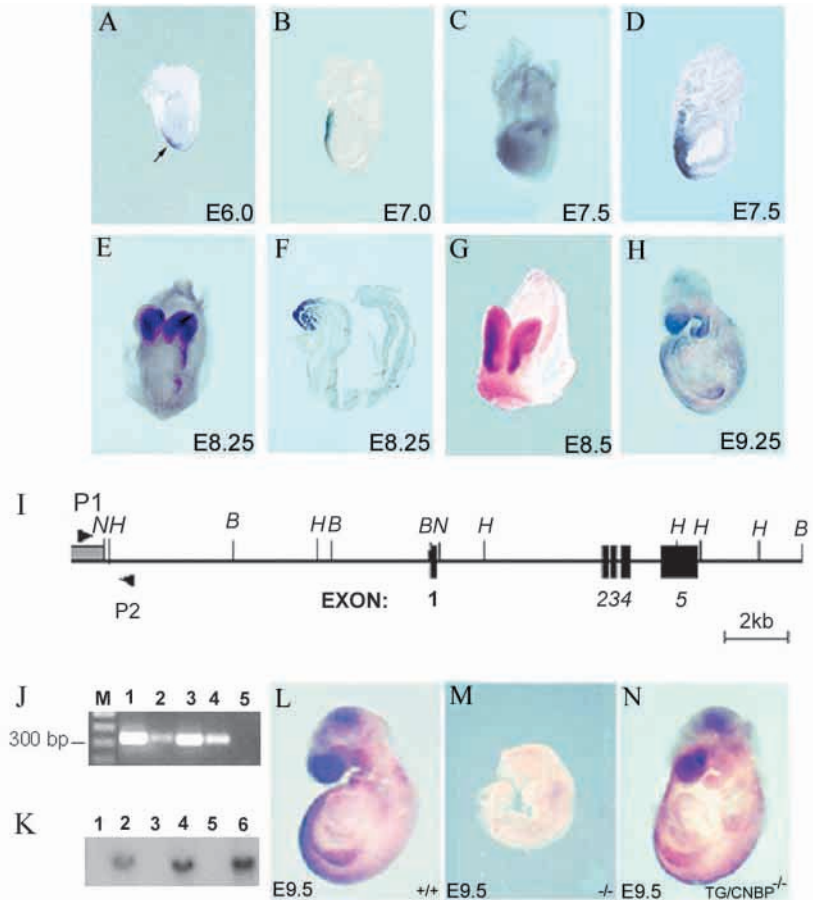
regions of E9.5 *Cnbp*^{-/-} embryos (Fig. 1J,K). However, the trunk and tail of the mutant embryos were relatively well formed.

Cnbp expression pattern in early embryonic development

To clarify the role of CNBP in mouse head development, we analyzed the expression of *Cnbp* at pre-gastrulation and gastrulation stages using whole-mount RNA in situ hybridization and tissue section immunostaining. We found that the expression of *Cnbp* during pregastrulation and

gastrulation stages was very dynamic. *Cnbp* was expressed in visceral endoderm located at the distal tip of the E6.0 embryo in pre-primitive streak stage (Fig. 2A). At E7.0, the early-primitive streak stage, *Cnbp* was expressed in the AVE (Fig. 2B). At E7.25, the late-primitive streak stage, CNBP protein was localized to the ADE, underlying the future forebrain, and in the overlying ANE, where the forebrain will form (Fig. 1P). At early neural plate stages (E7.5), *Cnbp* was expressed in the anterior axial mesendoderm, ADE and ANE (Fig. 2C,D). At 8-10 somites (E8.25-8.5), *Cnbp* expression became progressively

Fig. 2. Identification of early *Cnbp*-expression pattern and *Cnbp*-transgene rescue of forebrain defects in *Cnbp* mutants. (A-D) *Cnbp* expression was analyzed at pre-gastrulation, gastrulation and post-gastrulation stages by whole-mount in situ hybridization. (A) *Cnbp* is expressed at the visceral endoderm, anterior to the distal tip of the early embryo at early gastrulation (E6.0; arrow). (B) During primitive streak formation, at E7.0, *Cnbp* expression localizes to the AVE in the anterior midline from the proximal to the distal region. (C) *Cnbp* is expressed in anterior axial mesendoderm, ADE and ANE at late-primitive streak stage (E7.5). (D) Sagittal section of an embryo at an approximately similar stage to that shown in C, showing *Cnbp* expression in the anterior axial mesendoderm, ADE and ANE. (E-G) *Cnbp* is expressed in the anterior neural folds at 8-10 somite stages. (F) Sagittal section of an embryo at an approximately a similar stage to that shown in E, showing *Cnbp* expression in the ANE (forebrain) and head mesenchyme. (G) *Cnbp* continues to be expressed in the headfolds. (H) *Cnbp* is expressed in the forebrain at E9.25. Transcripts were also detected in the early facial prominences, including the first branchial arch, primitive maxillary region and early frontonasal area. Regions of expression other than the head include the limb bud and tail. (I) The *Cnbp* transgene comprising the 10 kb mouse *Cnbp* promoter, the entire *Cnbp* gene (11 kb) and a 300 bp vector DNA fragment (shaded region on left side) as a tag for genotyping. (J) Transgenic genotyping by PCR analysis using primers P1 and P2, described in I. Lane 5 shows control DNA from wild-type mice. The 300 bp fragment in lanes 1-4 represents recovery of transgenic embryos. (K) Transgenic genotyping by Southern blot analysis using the 300 bp vector DNA as probe. Wild-type embryos are represented in lanes 1, 3 and 5. Genomic DNA from transgenic embryos hybridizes to probe (lanes 2, 4 and 6). (L-M) Transgenic rescue of forebrain defects in *Cnbp* mutants. *Cnbp* expression in *Cnbp*^{+/+} wild-type embryo (L), *Cnbp*^{-/-} mutant (M) and TG/*Cnbp*^{-/-} (n=7) (N) embryos at E9.5. Embryo in M shows forebrain truncation, whereas the transgenic rescued embryo has a normal phenotype and a nearly identical expression pattern as the wild-type embryo (L,N). *Cnbp* begins to also be expressed in the midbrain shortly before E9.5 (L).



restricted to the headfold region (Fig. 2E-G). By E9.25, *Cnbp* was predominately expressed in the forebrain (Fig. 2H). The expression of *Cnbp* was also detected in midbrain by E9.5 (Fig. 2L). In addition to the head region, *Cnbp* expression was also detected in limb bud and tail at low level when organogenesis occurs (Fig. 2L). The expression pattern of *Cnbp* during early mouse development suggests that CNBP plays a role in patterning the anterior central nervous system (CNS), which is consistent with its role in forebrain formation.

Cnbp transgene rescue of forebrain defects in *Cnbp* mutants

To confirm that the forebrain truncation was indeed caused by a disruption of the *Cnbp* gene instead of by some unknown genetic or epigenetic mutations, we generated *Cnbp* transgenic (TG) mice to test whether the *Cnbp* transgene could rescue the forebrain defect in *Cnbp*^{-/-} mutants. The transgene contained a 10 kb *Cnbp* promoter and the entire 11 kb *Cnbp* gene (Fig. 2I). The TG mice were crossed with *Cnbp*^{+/-} mutants and the resultant progeny (TG/*Cnbp*^{+/-}) were then crossed with *Cnbp*^{+/-} mice. Litters were examined at E9.5. As previously described, *Cnbp*^{-/-} embryos showed forebrain truncations; however, transgene-positive *Cnbp*^{-/-} (TG/*Cnbp*^{-/-}) embryos

were normal (Fig. 2M,N). In situ hybridization revealed an almost identical *Cnbp*-expression pattern between wild-type and TG/*Cnbp*^{-/-} embryos (Fig. 2L,N). The forebrain truncation was rescued in TG/*Cnbp*^{-/-} embryos, which confirms that knockout of the *Cnbp* gene was responsible for the forebrain truncation phenotype.

Forebrain truncation in early *Cnbp* mutant embryos

We examined neuroectoderm formation and anteroposterior patterning in *Cnbp*^{-/-} embryos between 10-25 somite stages by the expression analysis of a number of CNS and mesoderm marker genes. *Bfl* mRNA, a marker for telencephalon forebrain, was entirely absent in E8.5 and E9.5 *Cnbp*^{-/-} embryos when compared with wild-type littermates (Fig. 3A,B,K,L). Loss of *Bfl* expression in mutant embryos at E8.5 suggests loss of the telencephalon. We examined the expression of other forebrain markers, such as *Hesx1* and *Six3*, which mark the diencephalon, to determine whether this tissue is also missing in the mutants. *Hesx1* and *Six3* were not detected in the mutants, indicating that diencephalon is also missing in the mutant embryos (Fig. 3C-F). To determine the anterior truncation level, engrailed1 (*En1*), a marker for posterior midbrain and anterior hindbrain was employed. *En1*

was expressed in the anterior region of both E9.0 normal and *Cnbp* mutant embryos (Fig. 3G,H), indicating that anterior hindbrain was not affected by the mutation. However, we could not determine whether midbrain is affected in the mutants from the analysis of *En1* expression. Another hindbrain marker, *Krox20* (*Egr2* – Mouse Genome Informatics), was detected in rhombomeres 3 and 5 of *Cnbp*^{-/-} embryos at E9.0 (Fig. 3I,J). Thus, the anterior hindbrain regions are present in homozygous mutants. We then used the mesoderm specific markers, *Mox1* and *Brachyury* (*T*) to determine whether trunk and tail development was affected. Both genes were expressed normally in homozygous mutants. *Mox1* expression was detected in paraxial mesoderm cells of E9.5 mutant embryos. *Mox1* expression was similar in the trunk regions of homozygous mutants as in their wild-type littermates (Fig. 3M,N). *T* expression was detected in the notochord and posterior (tail) mesoderm cells of both mutant E9.5 embryos, and in their wild-type littermates (Fig. 3O,P), indicating that notochord development is not affected in *Cnbp*^{-/-} homozygous embryos (Fig. 3P). Collectively, our expression analysis indicates that the *Cnbp* mutation results in forebrain truncation but does not affect posterior patterning beyond the midbrain, as development of hindbrain, trunk and tail of *Cnbp*^{-/-} embryos was essentially normal.

Defects of the AVE, ADE and ANE

In order to investigate the onset of the forebrain phenotypes, we analyzed the expression of a number of markers at early developmental stages when morphological abnormalities are not yet visible. We analyzed the expression of AVE markers *Hex* and *Lim1* at pre- and early-streak stages. At E6.0, AVE formation was initiated normally at the distal end of *Cnbp*^{-/-} embryos (Fig. 4A,B). The defects were first detected at mid-primitive streak stages (E6.5), when *Hex* expression did not complete a morphogenetic movement toward the proximal anterior region in *Cnbp*^{-/-} mutants when compared with wild-type littermates (Fig. 4C,D). The expression of *Lim1* in the anterior of mutants was also detected more distally when compared with that in wild-type embryos (Fig. 4E,F). Interestingly, the posterior expression of *Lim1* appeared to be more proximal, and closer to the extra-embryonic/embryonic junction in the mutant embryo compared with its expression pattern in wild-type embryos (Fig. 4E,F). The ectopic expression may be caused by the *Cnbp* mutation. In a similar case, ectopic expression of *Hesx1* was found throughout the ectodermal layer of the distal region of the egg cylinder at E6.75 *Cripto* mutants (Ding et al., 1998). Others have reported that *Otx2*-null mutant embryos also failed to execute movement of the AVE from the distal end to proximal region of

the embryo and that they lack anterior structures (Perea-Gomez et al., 2001). We conclude from these data, that CNBP is important for the correct localization of the AVE.

To understand further the developmental origins of the *Cnbp*^{-/-} phenotype, we investigated ADE induction (Lu et al., 2001). The ADE expresses many of the same genes as the AVE, such as *Hex* and *Cer1* (Martinez Barbera et al., 2000). The expression of *Hex* in *Cnbp*^{-/-} mutant embryos failed to occur at the late streak stage E7.5 (*n*=6) (Fig. 4K,L), indicating the ADE must be absent in *Cnbp*^{-/-} mutant embryos. *Cer1* is also normally expressed in the ADE at the late streak stage but was also absent in *Cnbp*^{-/-} mutant embryos (*n*=5) (Fig. 4M,N), which further confirms the lack of the ADE in *Cnbp*^{-/-} mutant

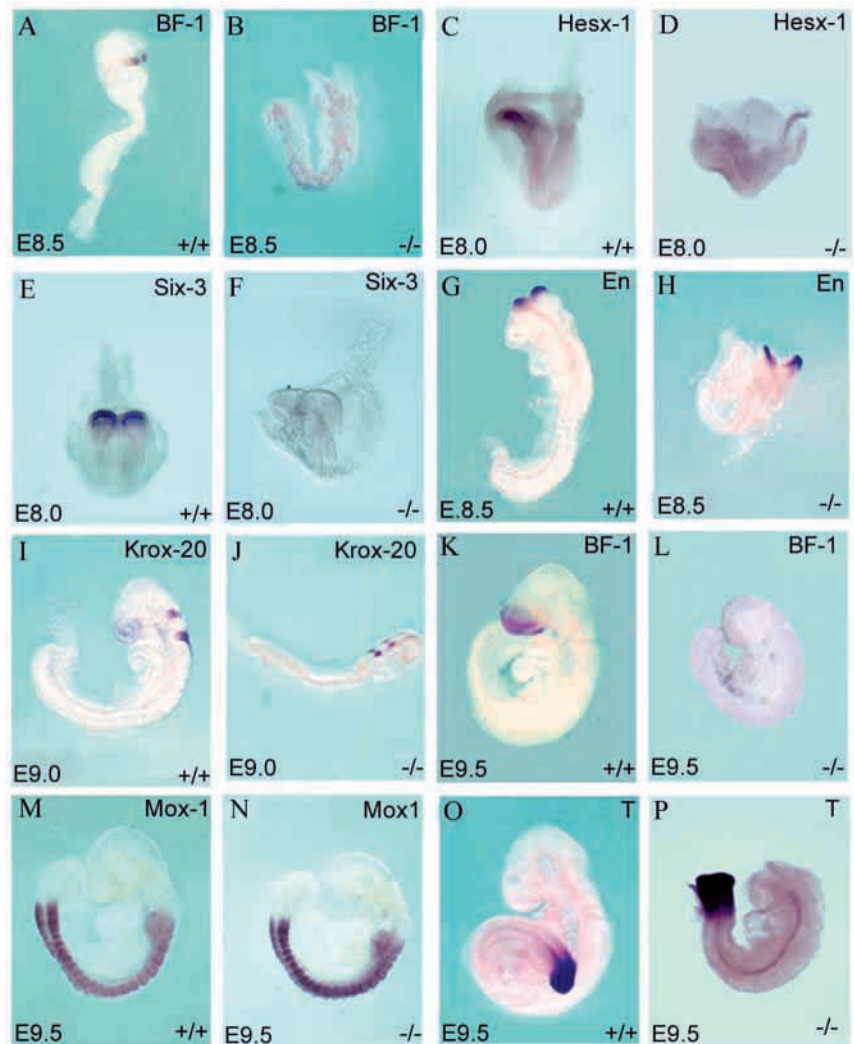


Fig. 3. Loss of forebrain in *Cnbp* mutants. (A,B,K,L) *Bfl* mRNA, a marker for the telencephalon was entirely absent in E8.5 (B) and E9.5 (L) *Cnbp*^{-/-} embryos (*n*=5). (C-F) *Hesx1* and *Six3* markers, used here to label the diencephalon, were entirely absent in E8.0 *Cnbp*^{-/-} embryos (D,F) when compared with wild-type littermates (C,E). (G,H) *En1*, a marker for midbrain and anterior hindbrain, is normally expressed in E8.5 wild-type and *Cnbp*^{-/-} mutant embryos. (I,J) Expression of *Krox20*, a marker for rhombomeres 3 and 5, is observed in E9.0 wild-type and *Cnbp*^{-/-} mutant embryos. (M,N) *Mox1* expression is normal in paraxial mesoderm cells in E9.5 *Cnbp*^{-/-} mutant when compared with their wild-type littermates. (O,P) *Brachyury* (*T*) expression is detected in the notochord and posterior mesoderm cells of mutant embryos at E9.5. *T* expression in tail was similar in homozygous mutants and their wild-type littermates.

embryos. Currently, we do not know why *Hex* and *Cer1* were not expressed in the mutants. The difference in expression of *Hex* and *Cer1* in mutants compared with wild-type embryos could be caused by a delay of development. In order to take into account the problem of developmental delay in the mutants, we then analyzed expression of these genes at E7.25 to determine whether the AVE is correctly positioned in the mutant embryos at this stage. Our results showed that at E7.25 stage, *Hex* and *Cer1* were expressed in the AVE and ADE of E7.25 wild-type embryos (Fig. 4G,I). By contrast, *Hex* mRNA was expressed at the distal tip in the E7.25 mutant embryos and this leads, in *Cnbp*^{-/-} E7.25 embryos, to the ectopic confinement of *Hex*-expressing cells to the region where the node is normally located (Fig. 4H). The expression of *Cer1* was also detected more distally when compared with that in wild-type embryos (Fig. 4J). Interestingly, the expression of *Hex* and *Cer1* in the ADE is not detected in the mutants at this stage (Fig. 4H,J). Mislocalization of the AVE and absence of the ADE indicate a defect in anterior displacement of the AVE instead of a developmental delay. The critical AVE movement could perhaps be a prerequisite for ADE formation. Its absence in *Cnbp*^{-/-} embryos supports this hypothesis.

To determine whether the induction of the ANE was affected in *Cnbp*^{-/-} embryos, we examined the expression of an ANE marker, *Otx2*, at E7.5. In all *Cnbp*^{-/-} mutants examined *Otx2* expression was undetectable (*n*=8) (Fig. 4O,P), which indicates that the cells destined for an anterior neural fate failed to form in the mutant embryos. Our data indicate that CNBP is required for ADE formation and anterior neural fate induction.

Defects of anterior mesendoderm (AME)

Recent transplantation experiments have demonstrated that a mixed graft of cells from the AVE, the anterior epiblast and the anterior streak can induce anterior neural genes (Tam and Steiner, 1999). In addition, removal of the ADE, together with prechordal plate and axial node derivatives, at the late gastrula stage results in truncation of the anterior neuroectoderm (Camus et al., 2000), indicating that a reciprocal interaction between these tissues is required for anterior patterning. To examine whether the *Cnbp* mutation affects the formation of anterior mesendoderm (AME), prechordal mesoderm, node and axial node derivatives, we analyzed the expression of a number of anterior mesendoderm markers, including *Lim1*, *T*, *Hnf3b*, *Gsc* and *Dkk1*, at primitive streak and early somite stages. *Lim1*, *T* and *Hnf3b* were all expressed in the node of wild-type embryos at E7.5 (Fig. 5A,C,E) (Ang et al., 1993; Monaghan et al., 1993). *Hnf3b* and *Lim1* were also expressed in midline cells anterior to the notochord, known as anterior mesendoderm or prechordal mesoderm cells (Fig. 5A,C). In homozygous mutants, all three genes were

expressed in the node and in the anterior region, but only a short distance from the node (Fig. 5B,D,F). This is in sharp contrast to wild-type embryos in which labeled head-process cells had migrated much farther anteriorly (Fig. 5B,D,F). In particular, the anterior-most midline expression of *Lim1* and *Hnf3b* in AME cells is missing in the mutants (Fig. 5B,D), indicating that the AME fails to develop. Later, during early somite stages, the absence of *Hnf3b* signal indicates defects in anterior axial mesoderm cells and the rostral portion of the

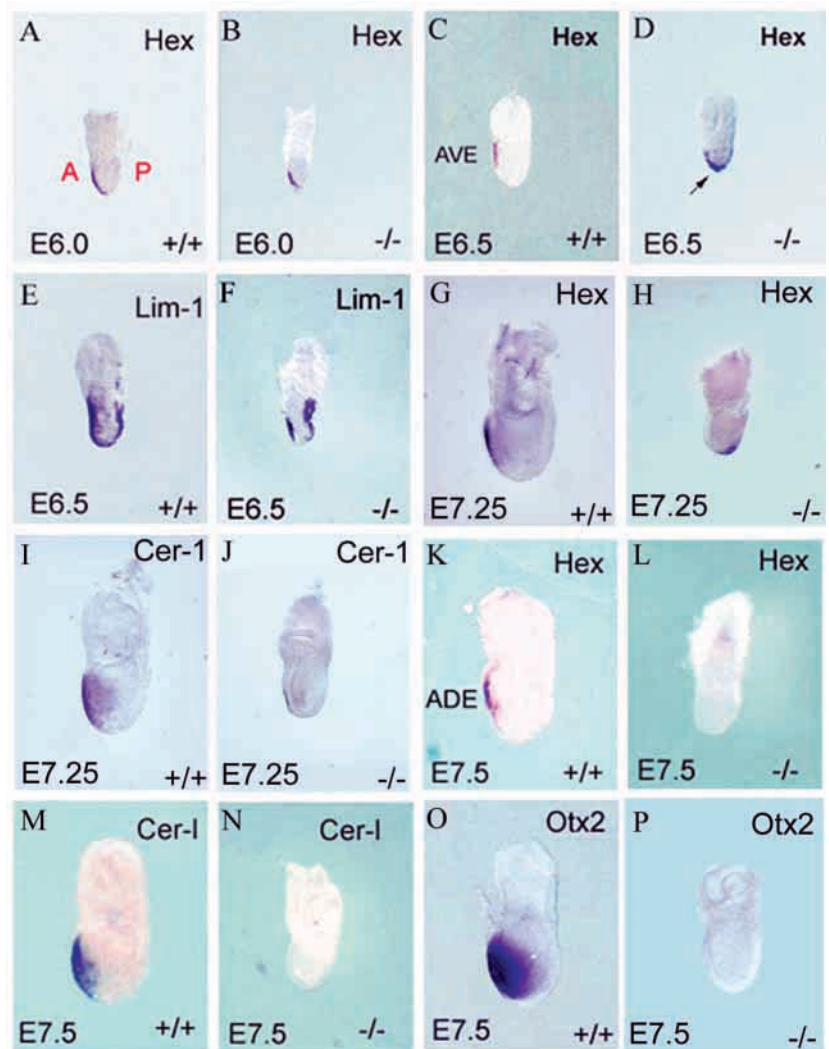


Fig. 4. Molecular analyses of the origins of the developmental defects in *Cnbp*^{-/-} mutants by whole-mount in situ hybridization analysis of marker genes. Lateral views of embryos are shown with anterior (A) to the left and posterior (P) to the right. (A,B) Whole-mount in situ hybridization with *Hex* probe at E6.0. *Hex* was expressed normally in the distal end of the epiblast of *Cnbp*^{-/-} mutant when compared with wild-type littermates. (C,D) *Hex* was expressed in the displaced AVE of E6.5 wild-type embryos but was retained near the distal end of the epiblast in the mutants (arrow). (E,F) *Lim1* is expressed in the AVE and the primitive streak of the E6.5 wild-type embryo; however, transcripts are more towards the distal end of the AVE in *Cnbp*^{-/-}. (G,H) *Hex* is expressed in the anterior definitive endoderm (ADE) and AVE of E7.25 wild-type embryos but is not detectable in E7.25 mutant embryos. (I,J) *Cer1* expression was undetectable in the ADE and AVE in E7.25 mutant embryos. (K,L) *Hex* is expressed in the ADE and ANE of E7.5 wild-type embryos but is not detectable in that of E7.5 mutant embryos. (M,N) *Cer1* expression was undetectable in the ADE and ANE in E7.5 mutant embryos. (O,P) Expression of *Otx2* in the ANE was not observed in mutant embryos.

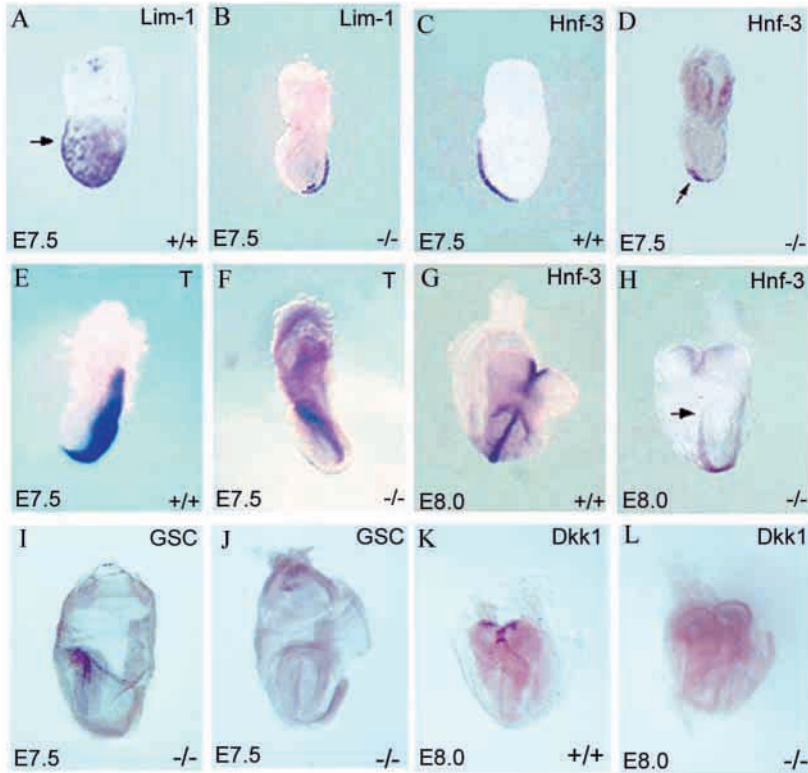


Fig. 5. Whole-mount RNA in situ hybridization staining of AME markers. (A,B) *Lim1* is expressed in the ADE and primitive streak at E7.5, but is undetected in the AME of mutant embryos. (C,D) *Hnf3b* is expressed in the node and prechordal mesoderm in wild-type embryo at E7.5, but only extends a short distance anteriorly from the node in mutant embryos (arrow). (E,F) *T* is expressed in the primitive streak of the wild-type and mutant embryos. In the mutants, *T* is only expressed at a short distance from the node. (G,H). At E8.0, *Hnf3b* expression in mutants is normal in the node and most of the midline but is absent from the anterior head and foregut pocket region. (I-L) Analysis of the of prechordal plate markers *Gsc* and *Dkk1* indicates that the E7.5 and E8.0 mutant embryos lack prechordal plate.

neural tube (Fig. 5G,H). The rostral expression of *Hnf3b* in the mutant embryo appears to be limited to the prospective hindbrain (Fig. 5H). This suggests that the midbrain development may also be affected in the mutant embryos. However, the potential defect in midbrain should be only a partial truncation based on the above morphological analysis (Fig. 1). The reduced *Lim1* and *Hnf3b* expression in the anterior embryo suggests a defect in the AME. To analyze this structure further, we used prechordal plate markers *Gsc* and *Dkk1* to assess prechordal plate development. *Gsc* and *Dkk1* were not expressed in E7.75 and E8.0 mutant embryos, indicating a defect in prechordal plate development (Fig. 5I-L). Although loss of *Cnbp* expression leads to defects in forebrain and midbrain development, the more posterior CNS is normal.

Reduced cell proliferation in anterior regions may account for defects in formation of the AVE, ADE, AME and ANE

We next investigated the cellular and molecular basis of the forebrain truncation defect in *Cnbp*^{-/-} embryos. The forebrain truncation may potentially result from defects in anterior neural cell differentiation, excess cell death, decreased cell proliferation or a combination of these processes in the developing forebrain region. Morphological and histological analysis indicated that the AME and ANE tissues of E7.5 *Cnbp*^{-/-} embryos were missing (Fig. 6A,B). Sagittal sections of E8.5 *Cnbp*^{-/-} embryos revealed defects in headfold formation and prechordal mesoderm formation (Fig. 6C,D). The rest of the body axis appeared normal. To compare the proliferative and apoptotic profiles in *Cnbp*^{-/-} and wild-type littermates, BrdU incorporation and TUNEL assays were performed on sections of E7.5 and E8.5 embryos. Wild-type

E7.5 and E8.5 embryos exhibit many BrdU-positive nuclei throughout the embryonic structures (Fig. 6E,G). By contrast, the mutants have fewer BrdU-positive nuclei in the ANE region (Fig. 6F,H). However, there is no significant difference in the number of BrdU-positive nuclei between the trunk region of wild-type and mutant embryos. The ratio of proliferating cells (BrdU-positive nuclei) to total cell number in the anterior of E7.5 embryos was calculated to be 84% for three wild-type embryos compared with 28% for three *Cnbp*^{-/-} mutant embryos (Fig. 6E,F,Q). As cells have been estimated to have a 10-12 hour division cycle during this period, a 10-20% decline in the proportion of S-phase cells during early post-implantation could result in a 25% decline in embryo size over a period of 1 day. The lack of cell proliferation may result in the observed reduction in size of the headfolds at E8.5 (Fig. 6H). TUNEL assays showed minimal apoptosis in normal and mutant E7.5 and 8.5 embryos (Fig. 6I-L), which suggests that programmed cell death does not contribute significantly, if at all, to the null phenotype. These findings indicated that the *Cnbp* mutation leads to a dramatic reduction in cell proliferation in the AME and ANE tissues, and headfold. To address further whether the impaired anterior movement of the AVE observed in *Cnbp* mutant embryos is related to defects in cell proliferation in AVE, we performed BrdU incorporation assays on E6.0 wild-type and mutant littermates. BrdU-positive nuclei were rarely seen in the prospective anterior region of the AVE in E6.0 mutant embryos (Fig. 6P). By contrast, the greatest density of BrdU-positive nuclei was observed in the anterior region of the AVE in normal E6.0 embryos (Fig. 6O). Our results suggest that reduced cell proliferation in anterior regions of *Cnbp* mutant embryos might account for defects in formation of the AVE, ADE, AME and ANE.

CNBP may control forebrain induction through Myc

CNBP was shown to regulate the CT element of the human *MYC* protooncogene through its binding to the element found in the *MYC* promoter (Michelotti et al., 1995). In addition to regulating cell proliferation and apoptosis, Myc can also promote differentiation of stem cells into transit-amplifying cells specific for the sebaceous and interfollicular epidermal lineages (Arnold and Watt, 2001; Gandarillas and Watt, 1997), and the *Myc*^{-/-} mutant has defects in development of anterior

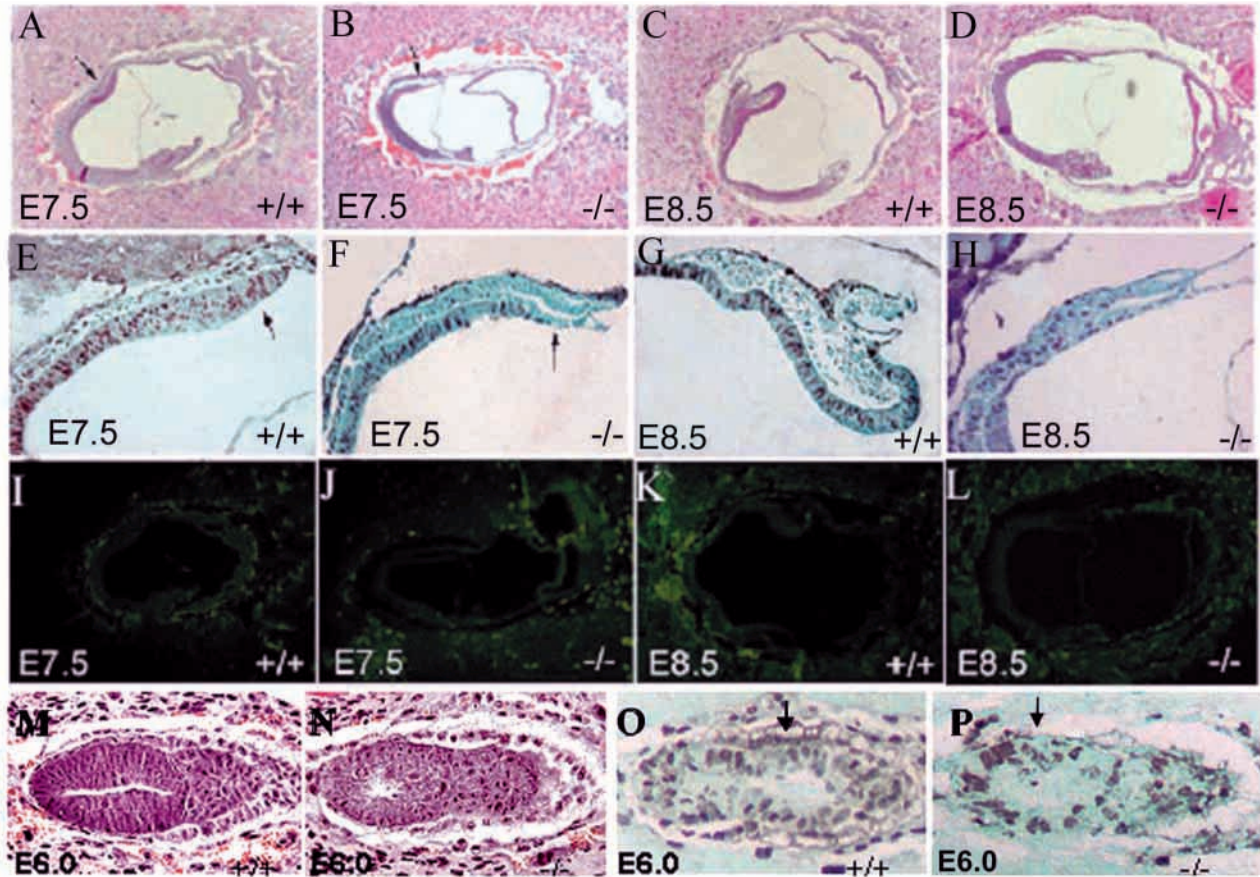


Fig. 6. Morphological and cellular basis of the forebrain defects in *Cnbp*^{-/-}. (A,B) Disorganization of the axial mesoderm and ANE region of cells (arrow) in E7.5 *Cnbp*^{-/-} mutants (A) compared with that (arrow) of wild-type littermates (B). (C,D) Lack of ANE and characteristic headfold structure in E8.5 *Cnbp*^{-/-} embryos compared with that of wild-type littermates. (E-H) Evidence for decreased proliferation rate in mutant head plate by BrdU incorporation analysis in adjacent sections of wild-type (E,G) and *Cnbp*^{-/-} mutant embryos (F,H). Arrow in F indicates that BrdU-positive nuclei were rarely seen in the anterior region of the mutant compared with that in wild-type embryo (arrow in E). Note that the head regions of wild-type embryos exhibit a high density of BrdU-positive nuclei throughout the axial mesoderm and ANE regions at E7.5, and in prechordal mesoderm and headfold regions at E8.5. The mutants showed much fewer BrdU-positive nuclei at the same regions. (I-L) TUNEL apoptosis assays in the histologically normal and mutant E7.5 and 8.5 embryos. TUNEL assays showed there was no significant difference of apoptosis in the anterior region of wild-type (I,K) and mutant (J,L) E7.5 and E8.5 embryos. (M-P) E6.0 *Cnbp*^{-/-} mutant embryos and wild-type littermates were examined for general morphology (M,N) and cell division using a BrdU incorporation assay (O,P). BrdU-positive nuclei in mutant embryos were absent in the AVE of E6.0 mutant head embryos (arrow in P). By contrast, the AVE region in normal E6.0 embryos showed the greatest density of BrdU-positive nuclei (arrow in O). (Q) Quantification of BrdU-positive nuclei in the anterior region of E7.5 embryos. The percent of BrdU-positive nuclei was 84% in wild-type embryos compared with 28% in null-mutant embryos. Error bars represent s.e., counts were made of three wild-type embryos (blue bar) and three null-mutant embryos (red bar). These values were determined to be statistically significant ($P < 0.001$).

structures (Davis et al., 1993; Gandarillas and Watt, 1997). These reports lead us to hypothesize that *Myc* is a downstream target gene of *Cnbp* during forebrain development, which may promote cell proliferation and differentiation in forebrain induction. We therefore examined the possible involvement of *Myc* in forebrain neuroectoderm induction and specification. We observed that *Myc* is expressed in anterior neuroectoderm at E7.25, and that the expression pattern of *Myc* in E8.5 and E9.5 mouse embryos was similar to that of *Cnbp* during forebrain development (Fig. 2C,E,H; Fig. 7A,C,E). Notably,

expression of *Myc* in the anterior neuroectoderm and the headfold region of E7.25 and E8.5 *Cnbp*^{-/-} mutant embryos was absent, whereas the expression of *Myc* in the allantois was normal (Fig. 7B,D). However, the loss of the anterior tissues by E8.5 and E9.5 could equally be the mechanism that results in reduced *Myc* expression. The regions where *Myc* expression was downregulated also showed reduced BrdU labeling, indicating that CNBP might regulate anterior cell proliferation through *Myc*.

To test whether CNBP regulates *Myc* expression at the

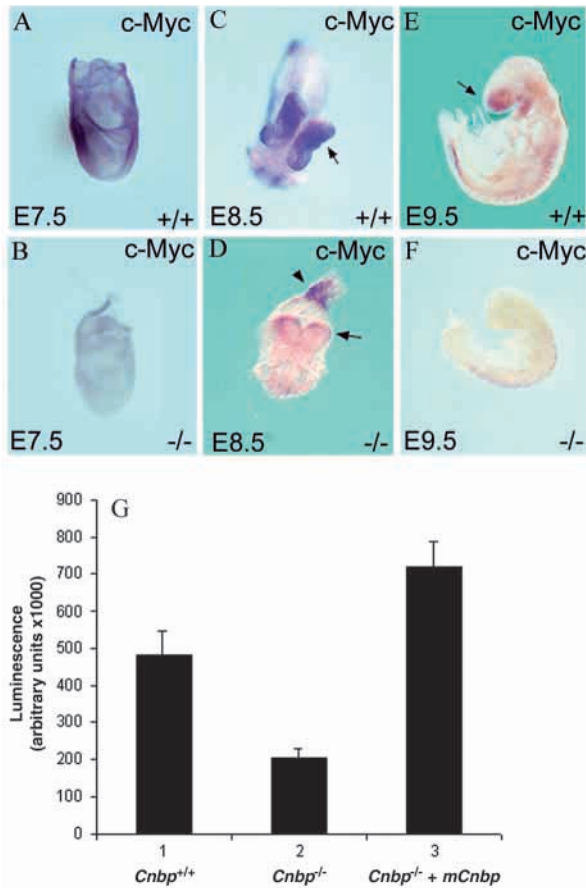


Fig. 7. CNBP positively regulates the endogenous expression of *Myc*. (A-D) *Myc* is normally abundantly expressed in the ANE at E7.25 (A) and in the neural folds (arrow, C) at E8.5, but is nearly undetectable in the neural folds (arrow, D) of *Cnbp* mutants. Expression in the allantois (arrowhead) is not affected in E8.5 mutant embryos. (E,F) At E9.5, *Myc* is expressed in the forebrain, as well as in the primitive facial prominences of wild-type embryos, but it was undetected in the anterior region of E9.5 mutant embryos. (G) CNBP upregulates *Myc* promoter activity in embryonic cells. *Cnbp*^{+/+} and *Cnbp*^{-/-} mouse embryonic fibroblast cells (MEFs) were transfected with *Myc* promoter-luciferase plasmid (columns 1 and 2) or co-transfected with a mouse *Cnbp*-expression plasmid into *Cnbp*^{-/-} cells (column 3). A lower level of *Myc* expression was observed in *Cnbp*^{-/-} embryonic fibroblasts compared with *Cnbp*^{+/+} cells. Transfection of *Cnbp*^{-/-} embryonic fibroblasts with the *Cnbp*-expression plasmid resulted in a *Myc* expression level higher than that found in *Cnbp*^{+/+} cells. Results represent luciferase activity related to galactosidase activity. Values are the mean \pm s.d. of triplicate experiments.

transcription level, we transfected wild-type and *Cnbp*^{-/-} mutant embryonic fibroblasts (MEF) with a *Myc* promoter-luciferase reporter plasmid (He et al., 1998). A lower level of luciferase activity was observed in *Cnbp*^{-/-} MEF than in wild-type cells (Fig. 7G). Co-transfection of *Cnbp*^{-/-} MEF with the luciferase reporter DNA and a mouse *Cnbp*-expression plasmid (CMV-CNBP) elevated *Myc* expression to a level higher than that seen in *Cnbp*^{+/+} cells (Fig. 7G). Therefore, we conclude that *Cnbp* expression enhances *Myc*-promoter activity. Although the mechanism by which *Cnbp* expression enhances *Myc* promoter activity during anterior patterning remains to be

elucidated, it is plausible that CNBP is one of the necessary transcription factors that bind to the *Myc* promoter to regulate its transcription.

DISCUSSION

Our work is the first to demonstrate the role of CNBP in rostral head formation during mouse embryonic development by generating *Cnbp* mutant mice, performing in vivo functional studies and transgenic mouse rescue, and characterizing the potential mechanism by which CNBP induces and specifies the forebrain through *Myc* expression and regulation of cell proliferation. Our results demonstrate that the *Cnbp* mutant mouse provides a valuable model for insight into anterior patterning related to AVE localization, ADE formation, neuralization of anterior ectoderm and forebrain induction.

A role for CNBP in head development

Our study has shown that ablation of *Cnbp* function in the mouse results in severe truncation of the forebrain. This finding provides direct genetic evidence that *Cnbp*, a zinc-finger protein, plays an essential and novel role in mouse forebrain development. De Robertis and colleagues have recently shown that mouse embryos carrying null mutations in the genes encoding BMP antagonists Noggin and Chordin fail to maintain a functional AVE and display forebrain defects (Bachiller et al., 2000). In addition, Mukhopadhyay and colleagues have recently shown that mouse embryos carrying null mutations in the genes encoding *Dkk1* display forebrain defects (Mukhopadhyay et al., 2001). Molecular marker analysis showed that expression of *Bfl*, *Hesx1* and *Six3* is completely absent; however, expression of *En1* is detected in *Dkk1*-mutant embryos. The identical expression pattern of the marker genes in both *Dkk1*- and *Cnbp*-mutant embryos indicates that both *Dkk1*- and *Cnbp*-mutant embryos show a similar forebrain phenotype. Although *Cnbp* is predominately expressed in the forebrain, *Cnbp* expression is also detected in midbrain region of E9.5 embryos. Moreover, E7.5 *Cnbp*-mutant embryos show a complete lack of *Otx2* expression, and the rostral level of *Hnf3b* expression in the mutant embryos appears to be limited to the hindbrain region, indicating a defect in midbrain tissues in the *Cnbp* mutants.

Cnbp expression in the early embryo is first noted in cells corresponding to a region of the early gastrulating embryo (at E6.0) where the AVE abuts the epiblast. However, no morphological defect can be detected in the *Cnbp*^{-/-} embryos prior to the early-streak stages. The defects were first detected at mid-primitive-streak stages (E6.5), when *Hex* expression did not complete a morphogenetic movement toward the proximal anterior region in *Cnbp*^{-/-} mutants when compared with wild-type littermates. The more distal *Hex* expression could be caused by a delay in development of the mutants. However, our results could not rule out the possibility of a delay in the development of mutants, based on the fact that: (1) *Hex* expression in E6.0 mutants is normal, which indicates the delay did not happen at this stage of development; (2) at E7.25, expression of *Hex* and *Cer1* was incorrectly positioned at the distal end in mutant embryos, which indicates defects in corresponding tissues, whereas we would expect that the AVE would persist and fully elongate, and that the ADE would be

induced if there was a delay in development; and (3) forebrain truncation in the E9.5 and newborn mutants is consistent with defects in the anterior tissue, whereas the trunk develops normally.

It is notable that *Otx2* expression is absent in *Cnbp* mutants at E7.5. As *Otx2*-null mutant embryos both failed to execute the movement of the AVE from the distal end to proximal region of the embryo (Perea-Gomez et al., 2001) and lack anterior structures (Ang et al., 1996), we suspect *Otx2* may act downstream of CNBP. However, in *Otx2* mutants the brain truncation was extended to anterior hindbrain as the expression of *En1* marker gene was not detected in *Otx2*-mutant embryos (Ang et al., 1996). Thus, the head defect phenotype in *Otx2*-mutant embryos is more severe than that in *Cnbp*-mutant embryos. The difference between the two mutations might be explained by residual *Otx2* protein or reduced *Otx2* expression in *Cnbp* mutants that was not detected by our *in situ* methods. An alternative possibility is that CNBP might only regulate *Otx2* expression in certain tissues and at specific stages. To address this question, mutant embryos at early stages will be analyzed in further studies. Nevertheless, the absence of *Otx2* expression in the prospective ANE cells of late-streak mutant embryos at E7.5 suggests that CNBP function is required for specification of the ANE during forebrain development. Forebrain patterning in the mouse is initiated by the inductive activity of the AVE and, subsequently, requires the function of the node-derived ADE (Ang et al., 1994; Shawlot et al., 1999; Tam and Steiner, 1999; Thomas and Beddington, 1996). The severe anterior phenotype of *Cnbp*^{-/-} embryos suggests that CNBP is a key factor in the head developmental process. However, it is not clear from this analysis whether CNBP is required in the AVE and/or the ADE for forebrain development. The generation of chimeric embryos composed of extra-embryonic and embryonic tissues of different genotypes would resolve this issue in future studies.

CNBP appears to regulate cell proliferation and tissue specification through *Myc* during forebrain induction

An abnormal constriction at the extra-embryonic/embryonic boundary is observed in *Cnbp*^{-/-} mutants. The constriction was also reported in *Otx2*, *Hnf3b* and *Lim1* mutants. However, the cause of the constriction remains unknown. Our cell proliferation data identify a substantial reduction in the cell proliferation of the AME and ANE, which is also associated with the loss of *Myc* expression in a tissue-specific manner where the constriction is observed. As no difference in apoptosis was evident between *Cnbp*^{-/-} and wild-type embryos, we conclude that the constriction arises as a result of reduced proliferation of the AVE and ANE during expansion of the ANE. The fact that CNBP upregulates CT elements in the *Myc* promoter and regulates cell proliferation highlights potential links between CNBP and *Myc*. In *Cnbp*^{-/-} embryos, CNBP appears to regulate proliferation through *Myc*. *Myc* is an important regulator of cell proliferation; however, others have recently shown that *Myc* is also involved in differentiation (Arnold and Watt, 2001; Gandarillas and Watt, 1997). *Myc* may be involved in ANE tissue specification. In homozygous *Cnbp* mutants, the lack of *Myc* may hinder neuralization in the anterior epiblast and, thus, further exacerbate the forebrain defect. Our data suggest a forebrain induction mechanism by

which CNBP induces the expression of *Myc*, which in turn stimulates cell proliferation and differentiation of the anterior epiblast and neuroectoderm cells during forebrain induction and specification. Although we propose that CNBP regulates forebrain formation through the *Myc* pathway, we could not rule out involvement of other CNBP target genes that have not yet been characterized. Interestingly, some *Myc*-null mutant embryos die at E10.5 with anterior neural fold truncation (Davis et al., 1993) whereas other *Myc* mutant embryos do not show obvious forebrain defects. One possible explanation is that CNBP targets a group of genes, including *Myc*, to regulate forebrain development. Another explanation is that an unknown factor may compensate for *Myc* loss in C57B1/6J and 129Sv hybrid or inbred 129Sv background (Davis et al., 1993). The role of *Myc* in forebrain formation remains to be investigated further.

The origins of forebrain phenotype of CNBP mutants are defects in the AVE and ADE tissues but not in the node and notochord

We find that AVE, ADE and ANE defects in *Cnbp*^{-/-} mice result in forebrain truncation initiated from early gastrulation stages. Other genes, such as *Lim1*, *Otx2*, *Nodal*, *Smad2*, *Foxh1*, *Arkadia*, *Hex*, *Oto*, *Dkk1*, *Hesx1*, *Nog* and *Chrd*, are also essential for murine head development (Episkopou et al., 2001; Hoodless et al., 2001; Shawlot et al., 1999; Yamamoto et al., 2001). However, the brain defects are considerably different among these mutants. Embryos homozygous for mutations in *Lim1*, *Otx2*, *Foxh1* or *Arkadia* exhibit truncations of the forebrain, midbrain and rostral hindbrain. By comparison, forebrain truncation in *Hex*^{-/-}, *Oto*^{-/-} and *Hesx1*^{-/-} embryos is relatively mild (Zoltewicz et al., 1999; Martinez Barbera et al., 2000). The defects observed in *Cnbp*^{-/-} embryos are clearly different from other mutants as *Cnbp*^{-/-} mutants showed complete forebrain truncation. The developmental origins of the defects are also considerably different among these mutants. The developmental defects in *Otx2* mutants originate from an inability of the AVE to complete its anteriorward movement and a failure to form the node, prechordal mesoderm, notochord and ADE. *Foxh1* and *Arkadia* mutants have normal AVE but impaired ADE, node and notochord. *Hex*^{-/-}, *Oto*^{-/-} and *Hesx1*^{-/-} mutants display absence or early regression of the ADE and normal AVE, node and notochord. Compared with other mutants that have brain defects, the developmental origin of the forebrain defects in *Cnbp*^{-/-} embryos is clearly unique. *Cnbp* mutants exhibit impaired AVE and ADE, with normal development of the node and notochord. The unique forebrain phenotype and developmental origin of the defects in *Cnbp* mutants indicate that the *Cnbp* mutation may affect a different genetic pathway when compared with any known mutation resulting in forebrain defects. Therefore, *Cnbp*^{-/-} embryos provide a unique and valuable mouse model for studying forebrain formation.

We are grateful to Ms Justine Dobeck for her excellent histology assistance and Dr S. P. Oh for his assistance with genomic gene cloning. We thank Dr Margaret A. Thompson for her assistance with transgenic mouse rescue work. We thank Dr Ryoji Moroi for his assistance with the manuscript. We thank Dr Kenneth W. Kinzler for the *Myc* promoter-luciferase plasmid, Dr Sarah Millar for the *Dkk1* probe and Dr Guillermo Oliver for the *Six3* probe. This work was

supported by NIH grant AR44741 (Y.-P. L.) and AR-48133-01 (Y.-P. L.).

REFERENCES

- Acampora, D., Mazan, S., Lallemand, Y., Avantaggiato, V., Maury, M., Simeone, A. and Brulet, P. (1995). Forebrain and midbrain regions are deleted in *Otx2*^{-/-} mutants due to a defective anterior neuroectoderm specification during gastrulation. *Development* **121**, 3279-3290.
- Acampora, D., Avantaggiato, V., Tuorto, F., Briata, P., Corte, G. and Simeone, A. (1998). Visceral endoderm-restricted translation of *Otx1* mediates recovery of *Otx2* requirements for specification of anterior neural plate and normal gastrulation. *Development* **125**, 5091-5104.
- Ang, S. L. and Rossant, J. (1994). HNF-3 beta is essential for node and notochord formation in mouse development. *Cell* **78**, 561-574.
- Ang, S. L., Wierda, A., Wong, D., Stevens, K. A., Cascio, S., Rossant, J. and Zaret, K. S. (1993). The formation and maintenance of the definitive endoderm lineage in the mouse: involvement of HNF3/forkhead proteins. *Development* **119**, 1301-1315.
- Ang, S. L., Conlon, R. A., Jin, O. and Rossant, J. (1994). Positive and negative signals from mesoderm regulate the expression of mouse *Otx2* in ectoderm explants. *Development* **120**, 2979-2989.
- Ang, S. L., Jin, O., Rhinn, M., Daigle, N., Stevenson, L. and Rossant, J. (1996). A targeted mouse *Otx2* mutation leads to severe defects in gastrulation and formation of axial mesoderm and to deletion of rostral brain. *Development* **122**, 243-252.
- Arnold, I. and Watt, F. M. (2001). c-Myc activation in transgenic mouse epidermis results in mobilization of stem cells and differentiation of their progeny. *Curr. Biol.* **11**, 558-568.
- Ayala-Torres, S., Johnson, B. H. and Thompson, E. B. (1994). Oxysterol sensitive and resistant lymphoid cells: correlation with regulation of cellular nucleic acid binding protein mRNA. *J. Steroid Biochem. Mol. Biol.* **48**, 307-315.
- Bachiller, D., Klingensmith, J., Kemp, C., Belo, J. A., Anderson, R. M., May, S. R., McMahon, J. A., McMahon, A. P., Harland, R. M., Rossant, J. et al. (2000). The organizer factors chordin and noggin are required for mouse forebrain development. *Nature* **403**, 658-661.
- Barklis, E., Mulligan, R. C. and Jaenisch, R. (1986). Chromosomal position or virus mutation permits retrovirus expression in embryonal carcinoma cells. *Cell* **47**, 391-399.
- Beddington, R. S. (1994). Induction of a second neural axis by the mouse node. *Development* **120**, 613-620.
- Beddington, R. S. and Robertson, E. J. (1999). Axis development and early asymmetry in mammals. *Cell* **96**, 195-209.
- Beddington, S. P. (1981). An autoradiographic analysis of the potency of embryonic ectoderm in the 8th day postimplantation mouse embryo. *J. Embryol. Exp. Morphol.* **64**, 87-104.
- Brennan, J., Lu, C. C., Norris, D. P., Rodriguez, T. A., Beddington, R. S. and Robertson, E. J. (2001). Nodal signalling in the epiblast patterns the early mouse embryo. *Nature* **411**, 965-969.
- Camus, A., Davidson, B. P., Billiards, S., Khoo, P., Rivera-Perez, J. A., Wakamiya, M., Behringer, R. R. and Tam, P. P. (2000). The morphogenetic role of midline mesendoderm and ectoderm in the development of the forebrain and the midbrain of the mouse embryo. *Development* **127**, 1799-1813.
- Cohen, M. M., Jr (1993). Sutural biology and the correlates of craniosynostosis. *Am. J. of Med. Genet.* **47**, 581-616.
- Covey, S. N. (1986). Amino acid sequence homology in gag region of reverse transcribing elements and the coat protein gene of cauliflower mosaic virus. *Nucl. Acids Res.* **14**, 623-633.
- Dattani, M. T., Martinez-Barbera, J. P., Thomas, P. Q., Brickman, J. M., Gupta, R., Martensson, I. L., Toresson, H., Fox, M., Wales, J. K., Hindmarsh, P. C. et al. (1998). Mutations in the homeobox gene *HESX1/Hesx1* associated with septo-optic dysplasia in human and mouse. *Nat. Genet.* **19**, 125-133.
- Davis, A. C., Wims, M., Spotts, G. D., Hann, S. R. and Bradley, A. (1993). A null c-myc mutation causes lethality before 10.5 days of gestation in homozygotes and reduced fertility in heterozygous female mice. *Genes Dev.* **7**, 671-682.
- De Dominicis, A., Lotti, F., Pierandrei-Amaldi, P. and Cardinali, B. (2000). cDNA cloning and developmental expression of cellular nucleic acid-binding protein (CNBP) gene in xenopus laevis. *Gene* **241**, 35-43.
- Deng, W., Stashenko, P., Chen, W., Liang, Y., Shimizu, K. and Li, Y. P. (2001). Characterization of mouse *Atp6i* gene, the gene promoter, and the gene expression. *J. Bone Miner. Res.* **16**, 1136-1146.
- Ding, J., Yang, L., Yan, Y. T., Chen, A., Desai, N., Wynshaw-Boris, A. and Shen, M. M. (1998). *Cripto* is required for correct orientation of the anterior-posterior axis in the mouse embryo. *Nature* **395**, 702-707.
- Episkopou, V., Arkell, R., Timmons, P. M., Walsh, J. J., Andrew, R. L. and Swan, D. (2001). Induction of the mammalian node requires Arkadia function in the extraembryonic lineages. *Nature* **410**, 825-830.
- Flink, I. L., Blitz, I. and Morkin, E. (1998). Characterization of cellular nucleic acid binding protein from *Xenopus laevis*: expression in all three germ layers during early development. *Dev. Dyn.* **211**, 123-130.
- Gandarillas, A. and Watt, F. M. (1997). c-Myc promotes differentiation of human epidermal stem cells. *Genes Dev.* **11**, 2869-2882.
- Harbers, K., Muller, U., Grams, A., Li, E., Jaenisch, R. and Franz, T. (1996). Provirus integration into a gene encoding a ubiquitin-conjugating enzyme results in a placental defect and embryonic lethality. *Proc. Natl. Acad. Sci. USA* **93**, 12412-12417.
- He, T. C., Sparks, A. B., Rago, C., Hermeking, H., Zawel, L., da Costa, L. T., Morin, P. J., Vogelstein, B. and Kinzler, K. W. (1998). Identification of c-MYC as a target of the APC pathway. *Science* **281**, 1509-1512.
- Hoodless, P. A., Pye, M., Chazaud, C., Labbe, E., Attisano, L., Rossant, J. and Wrana, J. L. (2001). FoxH1 (Fast) functions to specify the anterior primitive streak in the mouse. *Genes Dev.* **15**, 1257-1271.
- Jabs, E. W., Muller, U., Li, X., Ma, L., Luo, W., Haworth, I. S., Klisak, I., Sparkes, R., Warman, M. L., Mulliken, J. B. et al. (1993). A mutation in the homeodomain of the human *MSX2* gene in a family affected with autosomal dominant craniosynostosis. *Cell* **75**, 443-450.
- Kimura, C., Yoshinaga, K., Tian, E., Suzuki, M., Aizawa, S. and Matsuo, I. (2000). Visceral endoderm mediates forebrain development by suppressing posteriorizing signals. *Dev. Biol.* **225**, 304-321.
- Konicek, B. W., Xia, X., Rajavashisth, T. and Harrington, M. A. (1998). Regulation of mouse colony-stimulating factor-1 gene promoter activity by AP1 and cellular nucleic acid-binding protein. *DNA Cell Biol.* **17**, 799-809.
- Lawson, K. A. and Pedersen, R. A. (1987). Cell fate, morphogenetic movement and population kinetics of embryonic endoderm at the time of germ layer formation in the mouse. *Development* **101**, 627-652.
- Lawson, K. A., Meneses, J. J. and Pedersen, R. A. (1991). Clonal analysis of epiblast fate during germ layer formation in the mouse embryo. *Development* **113**, 891-911.
- Li, E., Bestor, T. H. and Jaenisch, R. (1992). Targeted mutation of the DNA methyltransferase gene results in embryonic lethality. *Cell* **69**, 915-926.
- Li, Y. P., Chen, W., Liang, Y., Li, E. and Stashenko, P. (1999). *Atp6i*-deficient mice exhibit severe osteopetrosis due to loss of osteoclast-mediated extracellular acidification. *Nat. Genet.* **23**, 447-451.
- Lu, C. C., Brennan, J. and Robertson, E. J. (2001). From fertilization to gastrulation: axis formation in the mouse embryo. *Curr. Opin. Genet. Dev.* **11**, 384-392.
- Martinez Barbera, J. P., Clements, M., Thomas, P., Rodriguez, T., Meloy, D., Kioussis, D. and Beddington, R. S. (2000). The homeobox gene *Hex* is required in definitive endodermal tissues for normal forebrain, liver and thyroid formation. *Development* **127**, 2433-2445.
- Matsuo, I., Kuratani, S., Kimura, C., Takeda, N. and Aizawa, S. (1995). Mouse *Otx2* functions in the formation and patterning of rostral head. *Genes Dev.* **9**, 2646-2658.
- Michelotti, E. F., Tomonaga, T., Krutzsch, H. and Levens, D. (1995). Cellular nucleic acid binding protein regulates the CT element of the human c-myc protooncogene. *J. Biol. Chem.* **270**, 9494-9499.
- Monaghan, A. P., Kaestner, K. H., Grau, E. and Schutz, G. (1993). Postimplantation expression patterns indicate a role for the mouse forkhead/HNF-3 alpha, beta and gamma genes in determination of the definitive endoderm, chordamesoderm and neuroectoderm. *Development* **119**, 567-578.
- Moon, R. T. and Kimelman, D. (1998). From cortical rotation to organizer gene expression: toward a molecular explanation of axis specification in *Xenopus*. *BioEssays* **20**, 536-545.
- Mukhopadhyay, M., Shtrom, S., Rodriguez-Esteban, C., Chen, L., Tsukui, T., Gomer, L., Dorward, D. W., Glinka, A., Grinberg, A., Huang, S. P. et al. (2001). *Dickkopf1* is required for embryonic head induction and limb morphogenesis in the mouse. *Dev. Cell* **1**, 423-434.
- Nomura, M. and Li, E. (1998). *Smad2* role in mesoderm formation, left-right patterning and craniofacial development. *Nature* **393**, 786-790.

- Perea-Gomez, A., Lawson, K. A., Rhinn, M., Zakin, L., Brulet, P., Mazan, S. and Ang, S. L.** (2001). Otx2 is required for visceral endoderm movement and for the restriction of posterior signals in the epiblast of the mouse embryo. *Development* **128**, 753-765.
- Piotrowska, K. and Zernicka-Goetz, M.** (2001). Role for sperm in spatial patterning of the early mouse embryo. *Nature* **409**, 517-521.
- Rajavashisth, T. B., Taylor, A. K., Andalibi, A., Svenson, K. L. and Lusic, A. J.** (1989). Identification of a zinc finger protein that binds to the sterol regulatory element. *Science* **245**, 640-643.
- Shawlot, W. and Behringer, R. R.** (1995). Requirement for Lim1 in head-organizer function. *Nature* **374**, 425-430.
- Shawlot, W., Wakamiya, M., Kwan, K. M., Kania, A., Jessell, T. M. and Behringer, R. R.** (1999). Lim1 is required in both primitive streak-derived tissues and visceral endoderm for head formation in the mouse. *Development* **126**, 4925-4932.
- Shen-Li, H., O'Hagan, R. C., Hou, H., Jr, Horner, J. W., Lee, H. W. and DePinho, R. A.** (2000). Essential role for Max in early embryonic growth and development. *Genes Dev.* **14**, 17-22.
- Tam, P. P. and Beddington, R. S.** (1992). Establishment and organization of germ layers in the gastrulating mouse embryo. *Ciba Found. Symp.* **165**, 27-41.
- Tam, P. P. and Steiner, K. A.** (1999). Anterior patterning by synergistic activity of the early gastrula organizer and the anterior germ layer tissues of the mouse embryo. *Development* **126**, 5171-5179.
- Thomas, P. and Beddington, R.** (1996). Anterior primitive endoderm may be responsible for patterning the anterior neural plate in the mouse embryo. *Curr. Biol.* **6**, 1487-1496.
- van Heumen, W. R., Claxton, C. and Pickles, J. O.** (1997). Sequence and tissue distribution of chicken cellular nucleic acid binding protein cDNA. *Comp. Biochem. Physiol. B Biochem. Mol. Biol.* **118**, 659-665.
- Waldrip, W. R., Bikoff, E. K., Hoodless, P. A., Wrana, J. L. and Robertson, E. J.** (1998). Smad2 signaling in extraembryonic tissues determines anterior-posterior polarity of the early mouse embryo. *Cell* **92**, 797-808.
- Warden, C. H., Krisans, S. K., Purcell-Huynh, D., Leete, L. M., Daluiski, A., Diep, A., Taylor, B. A. and Lusic, A. J.** (1994). Mouse cellular nucleic acid binding proteins: a highly conserved family identified by genetic mapping and sequencing. *Genomics* **24**, 14-19.
- Yamamoto, M., Meno, C., Sakai, Y., Shiratori, H., Mochida, K., Ikawa, Y., Saijoh, Y. and Hamada, H.** (2001). The transcription factor FoxH1 (FAST) mediates Nodal signaling during anterior-posterior patterning and node formation in the mouse. *Genes Dev.* **15**, 1242-1256.
- Zoltewicz, J. S., Plummer, N. W., Lin, M. I. and Peterson, A. S.** (1999). Oto is a homeotic locus with a role in anteroposterior development that is partially redundant with Lim1. *Development* **126**, 5085-5095.